Brazilian Journal of Physics
ISSN: 0103-9733
luizno.bjp@gmail.com
Sociedade Brasileira de Física
Brasil

Yaghobi, Mojtaba; Reza Niazian, Mohammad
Inelastic Electron Transport Through a Carbon Fullerene Junction
Brazilian Journal of Physics, vol. 44, núm. 6, 2014, pp. 687-696
Sociedade Brasileira de Física
Sâo Paulo, Brasil

Braz J Phys (2014) 44:687–696
DOI 10.1007/s13538-014-0263-1

CONDENSED MATTER

Inelastic Electron Transport Through a Carbon Fullerene Junction

Mojtaba Yaghobi · Mohammad Reza Niazian

Received: 26 May 2014 / Published online: 30 September 2014

Abstract Effects of inelastic electron–phonon interactions and different contact geometries on the electron transport and thermoelectric properties of the C_{60} molecule are studied by Green's function theory within the framework of polaron transformation. It is seen that the current (I_e) and energy flux (I_Q) values with respect to the contact types are ordered as $I_{e/q}(C_1)<I_{e/q}(C_6)<I_{e/q}(C_5)$. The results reveal that the thermopower–energy curves have strictly monotonic character which show the staircase structures. Their stair numbers depend on contact types and presence of electron–phonon interactions. It is shown that the oscillatory behavior of thermal conductance is dramatically dependent on contact types and e–p interactions. Also, the values of the dimensionless figures of merit (ZT_0) lie in the interval $[0.322 \times 10^{-7}, 0.194 \times 10^{-3}]$, and effect of contact types is small on the values of ZT_0s.

Keywords Thermoelectric effect · Polaronic transport · Electron–phonon interaction · Fullerene junction

1 Introduction

In recent years, the experimental and theoretical studies of molecular junctions have received much attention due to the number of novel and promising physical characteristics such as conductance quantization, the nonlinear current–voltage characteristics, negative differential resistance (NDR), giant magnetoresistance (GMR), tunnel magnetoresistance (TMR), and the Kondo effect [1–10]. These physical characteristics have found important applications in prototype devices as the readheads of modern hard disk drives, nonvolatile semiconductor memory, information processing, molecular switches, logic cells, and memory and other electronic applications on the nanoscale [11, 12]. The studies indicated that the quantum nature of the molecular system, electronic properties of the electrodes near the Fermi energy level, and the strength of molecule-to-electrodes coupling affect the electron transport [13].

The effects of thermal broadening and inelastic scattering due to the electron–phonon interactions should be considered in calculations because the thermal effects are present in experiments. The temperature-dependent thermoelectric power (TEP) of nanostructures was studied both theoretically and experimentally [14–17]. In the linear response regime, the impact of electron–phonon interaction on the thermoelectrical properties of a quantum dot device was investigated by Koch et al. [18].

Thermopower and thermal conductance of atomic sized metallic contacts, 1D Wires, single-electron transistor, and double quantum well were studied in recent years [19–22].

2 Theoretical Methods

In this research, we consider that a system consists of a C_{60} molecule contacted by single and multiple atoms to two metallic electrodes with finite cross sections, simple cubic structure, and square cross section. In the semi-infinite electrodes described by the wide-band (WB) model [26], only the central site at the cross section is connected to the molecule.

The model of such a structure is shown schematically in Fig. 1a–c. The system Hamiltonian is expressed as follows:

$$\widehat{H} = \widehat{H}_L + \widehat{H}_R + \widehat{H}_C + \widehat{H}_T, \quad (1)$$

M. Yaghobi (✉) · M. R. Niazian
Ayatollah Amoli Branch, Islamic Azad University, Amol, Iran
e-mail: mojtabayaghobii@gmail.com

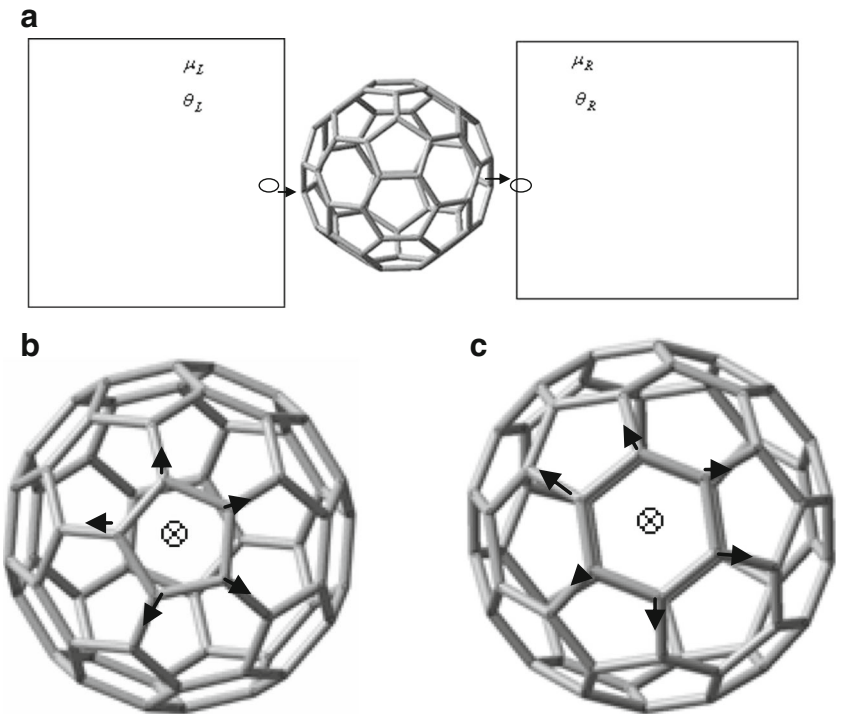

Fig. 1 **a** Geometric configureuration of the carbon molecular junction. A C_{60} molecule connected to two reservoirs via potential barriers. Schematic view of **b** five and **c** six atomic contacts of C_{60} molecule. The central site of contacts is depicted by a *cross inside a circle*. The *vector arrows* (→) indicate the current directions of each bond of the single and multiple contacts

where $\widehat{H}_L$ and $\widehat{H}_R$ are the Hamiltonians of the left (L) and right (R) electrodes, $\widehat{H}_C$ describes the channel Hamiltonian, and $\widehat{H}_T$ is the coupling between the electrodes and central part. Hamiltonian of electrodes can be written as

$$\widehat{H}_\alpha = \sum_{(i_\alpha, j_\alpha)} \left(\varepsilon_\alpha \delta - t_{i_\alpha, j_\alpha}\right) c_{i_\alpha}^{+} c_{j_\alpha} \quad (\alpha = L, R) \tag{2}$$

Here, ε_α is the on-site energy of the electrodes and will be set to 0. The coupling Hamiltonian is described as

$$\widehat{H}_T = \sum_{\alpha=\{L,R\}} \sum_{(i_\alpha, j_C)} \left(-t'_\alpha\right)\left(c_{i_\alpha}^{+} d_{j_C} + h.c.\right). \tag{3}$$

The Hamiltonian of the central part can be extended as [24]

$$\widehat{H}_C = \sum_i \varepsilon_i d_i^{+} d_i + \widehat{H}_{SSH}, \tag{4}$$

with

$$H_{SSH} = \sum_{\langle i,j \rangle} \left[-t_0 + \sum_k \lambda_{i,j}^k \left(a_k^{+} + a_k\right)\right]\left(d_i^{+} d_i + H.C.\right) + \sum_k h\omega_k a_k^{+} a_k \tag{5}$$

Here, the hopping integrals t_0 and t' are the nearest-neighbor hopping integrals, d_i^{+} or c_i^{+} (d_i or c_i) is the creation (annihilation) operator of the π electron at site i, while a_k and a_k^{+} are phonon creation and annihilation. The sum over $\langle i,j \rangle$ is taken over nearest-neighbor pair $\langle i,j \rangle$. ε_i is the on-site energy where it is equal to the gate voltage.

In addition, the second term of $\widehat{H}_{ssh}$ is the electron–phonon interaction with the coupling strength given by $\lambda_{i,j}^k$. Finally, the third term of $\widehat{H}_{ssh}$ indicates the purely phononic energy with phonon frequency ω_k for the k-mode. The phonon modes with energies $\Omega = h\omega_k = 0.13$ and $0.10eV$ were considered in calculations by solving the familiar eigenvalue problem [23]:

$$\sum_j V_{i,j} \overrightarrow{r}_j^k = -m_i \omega_k^2 \overrightarrow{r}_i^k, \tag{6}$$

where the sum over j is just over the nearest neighbors of atom i with mass m_i. Also, the atoms in the leads are assumed fixed in their static positions. The effective spring coupling between the nearest neighbors of atoms of the molecule is chosen to be $V_{i,j} = K = 49.7$ eV/$\mathring{A}^2$ [24]. $\overrightarrow{r}_i^k$ is the displacement from equilibrium position of the i atom.

The electron states in molecule and leads in terms of the direct product states composed of single-electron states and n-phonon Fock states are expanded, respectively, as [25]

$$|i, m\rangle = d_i^{+} \frac{(a^{+})^m}{m!}|0\rangle \text{ and } |i, m\rangle = c_i^{+} \frac{(a^{+})^m}{m!}|0\rangle. \tag{7}$$

In the new representation, $\widehat{H}_c$ and $\widehat{H}_T$ can be rewritten in the forms

$$H_C = \sum_{i,m} (\varepsilon_i + m\Omega)|i,m\rangle\langle i,m|$$

$$+ \sum_{\langle i,j\rangle,m} \left[-t_0|i,m\rangle\langle j,m| + \lambda\sqrt{m+1}(|i,m+1\rangle\langle j,m| + |i,m\rangle\langle j,m+1|)\right] \tag{8}$$

and

$$\widehat{H}_T = \sum_{\alpha=\{L,R\}} \sum_{(i_\alpha,j_C),\sigma} \left[-t'_\alpha|i_\alpha,m\rangle\langle j_C,m|\right]. \tag{9}$$

The incoming channel m is connected with outgoing channel n in terms of transmission probability of the individual transitions $T_{m,n}(\varepsilon,V_b) = tr\left[\widehat{\Gamma}_L\widehat{G}^R_{m+1,n+1}\widehat{\Gamma}_R\widehat{G}^A_{m+1,n+1}\right]$. The transmission function depends on energy (ε) and bias voltage (V_b) where $G^{R,A}_C$ are the retarded and advanced Green's functions and the coupling function $\Gamma_{L,R}$ are the linewidth functions of the left and right electrodes, respectively. Also, electron energies are constrained by the energy conservation law as $\varepsilon_{in}+mh\omega=\varepsilon_{out}+nh\omega$. It is obvious that the elastic contributions can be obtained by imposing the constraint of elastic transitions, where $\varepsilon_{in}=\varepsilon_{out}$ or more precisely $m=n$.

In the nonlinear response regime, both the total current (I_e) flowing through the junction and the energy flux (I_Q) can be expressed as [25]

$$I_e(V_b) = \frac{2e}{h}\int_{-\infty}^{\infty}\sum_{m,n}\left[P_m f_L^m\left(1-f_R^n\right) - P_n f_R^n\left(1-f_L^m\right)\right]T_{m,n}(\varepsilon,V_b)d\varepsilon \tag{10}$$

$$I_Q(V_b) = \frac{2}{h}\int_{-\infty}^{\infty}\sum_{m,n}\left[P_m f_L^m\left(1-f_R^n\right) - P_n f_R^n\left(1-f_L^m\right)\right]T_{m,n}(\varepsilon,V_b)\varepsilon d\varepsilon\,. \tag{11}$$

Here, $f^m_{L/R}(\varepsilon,V_b)=[\exp[\beta_{L/R}(\varepsilon+mh\omega-\mu_{L/R})]+1]$ are the Fermi–Dirac distribution functions of the left and right electrodes, $\mu_{L/R} = E_f \pm \frac{1}{2}eV_b$ are the electrochemical potentials of the left and right electrodes, $P_m=[1-\exp(-\beta_R h\omega)]\exp(-\beta_R mh\omega)$ *is the Boltzmann distribution function, h is the Planck's constant, and e is the electron charge.*

In the presence of the bias voltage, the Green's function of system is evaluated from the effective Hamiltonian of the molecule (H_C) and self-energy functions (Σ) as [13]

$$G^{R/A}(\varepsilon,V_b) = \left[(\varepsilon \pm i\eta)\hat{I} - H_C - \sum_L(\varepsilon,V_b) - \sum_R(\varepsilon,V_b)\right]^{-1}. \tag{12}$$

Here, $\eta=0^+$ is a positive infinitesimal constant. By applying the wide band approximation, the self-energy matrixes for left (L) and right (R) leads are defined as [26]

$$\sum_\alpha = 2i\Gamma_\alpha = -\widehat{\tau}^{+}_{\alpha C}\widehat{g}_\alpha\widehat{\tau}_{\alpha C}, \quad (\alpha = L,R) \tag{13}$$

where $\widehat{\tau}$ is the hopping matrix that couples the molecule to the leads and its elements are independent of energy. $\widehat{g}_\alpha = i\pi\rho_\alpha$ is the surface Green's function of the uncoupled α-electrode and ρ_α is the density of states in the α-electrode in the Fermi energy.

Around the linear response region, the thermoelectric coefficients are given through the following expressions [25, 27]:

$$\begin{pmatrix} I_e \\ I_Q \end{pmatrix} = \begin{pmatrix} e^2L_0 & ek_B\beta_R L_1 \\ eL_1 & k_B\beta_R L_2 \end{pmatrix}\begin{pmatrix} V \\ \delta\theta \end{pmatrix}. \tag{14}$$

These expressions indicate that the charge and energy fluxes are directly proportional to the chemical potential difference $V = \frac{(\mu_L-\mu_R)}{e}$ and the temperature difference $\Delta\theta=(\theta_L-\theta_R)$.

The coefficients L_n (n=0, 1, and 2) are defined as [25, 27]

$$L_n = \frac{2}{h}\int_{-\infty}^{\infty}\sum_{m,n}\left[-\varepsilon'\right]^n\left(-\frac{\partial f^m(\varepsilon-\varepsilon')}{\partial\varepsilon}\right)P_m T_{m,n}(\varepsilon')d\varepsilon'\,. \tag{15}$$

Here, $F_T(\varepsilon) = \left(-\frac{\partial f^m(\varepsilon)}{\partial\varepsilon}\right) = \frac{\beta_R}{4}\mathrm{sech}^2\left(\frac{\beta_R}{2}\varepsilon\right)$ with $\beta_R^{-1}=k_B\theta_R$ is responsible for the broadening of peaks of thermoelectric coefficients. k_B is the Boltzmann constant and $\theta_{L/R}$ are the finite temperatures of left and right electrodes.

The thermopower S can be found as

$$S = \left(-\frac{\Delta V}{\Delta T}\right)_{I_e=0} = \frac{k_B\beta_R L_1}{eL_0}\,. \tag{16}$$

Another important quantity is the conventional thermal conductance of electrons at zero electron current which is given through the following expressions:

$$\kappa = \left(-\frac{I_Q}{\Delta T}\right)_{I_e=0} = e\left[-SL_1 + \frac{k_B}{e}\beta_R L_2\right]. \tag{17}$$

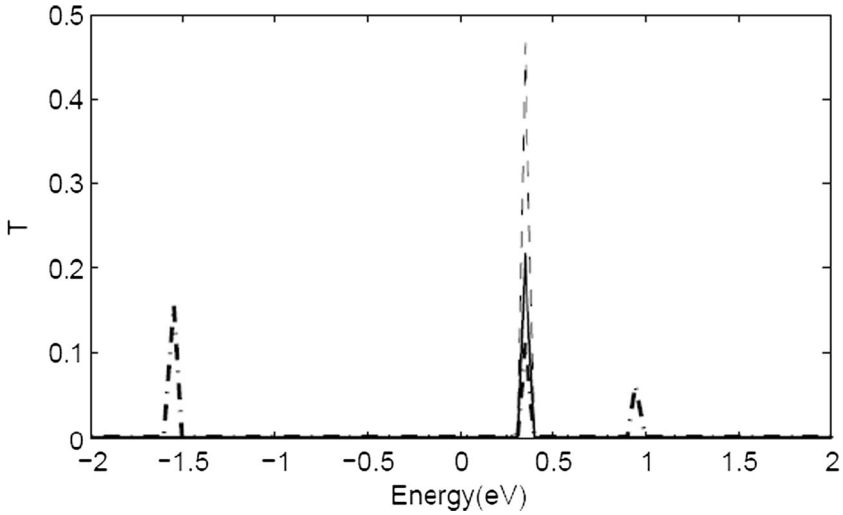

Fig. 2 The total transmission probability of C_{60} molecule as a function of electron energy for one (–.), five (—), and six (__) atomic contacts at V_b=0.0 V and in absence of e–p interactions

3 Results and Discussion

The C_{60} molecule can be coupled through an arbitrary number of carbon atoms to two leads that are taken symmetric with respect to the plane through the center of mass of the molecule. C_{60} is a beautifully symmetric molecule which belongs to the icosahedral symmetry and is formed of 12 pentagons and 20 hexagons having the same edge dimension close to that of the C–C bond in graphite. Therefore, the direction of the molecule changes the number of contact points when two electrodes are connected to the C_{60} molecule. Thus, single or multiple contacts may occur. In this study, the coupling through two facing atoms (Fig. 1a) or pentagons (Fig. 1b) or hexagons (Fig. 1c) of the C_{60}molecule to the central site at the cross section of each electrode will be considered. Here, we adopt the following parameters of the model (given in eV): ε_F=−1, ε_0=0, $\rho_L^{-1}=\rho_R^{-1}$=14.3, $t_L'=t_R'$=0.24, t_0=2.5, $\beta_L^{-1}=k_B\theta_L$=0.015, $\beta_R^{-1}=k_B\theta_R$=0.025, and $\lambda_{i,j}^k=\lambda$. For the parameters involved in the present paper, the maximum number of allowed phonon quanta $m_{\max}$=3 is selected to obtain fully converged results.

It should be pointed out that the values of current are displayed as a function of the applied bias voltage for all systems. The bias voltages are in the range from −4.0 to 4.0 V in steps of 0.1 V, which is reasonable in practical experimental measurements. All the calculations are performed in the weak coupling regime ($t_{L/R}'<<t_0$) by using wide-band (WB) approximation. Here, our attention has been concentrated on the effect of the inelastic scattering process in tunneling, and all the interactions between charge carriers are neglected. Therefore, a nonperturbative method based on Green's function theory within the framework of polaron transformation (GFT-PT) has been used in this work [26]. Also, effects of phase decoherence processes in the treatment of the electron–phonon exchange, the Coulomb interactions

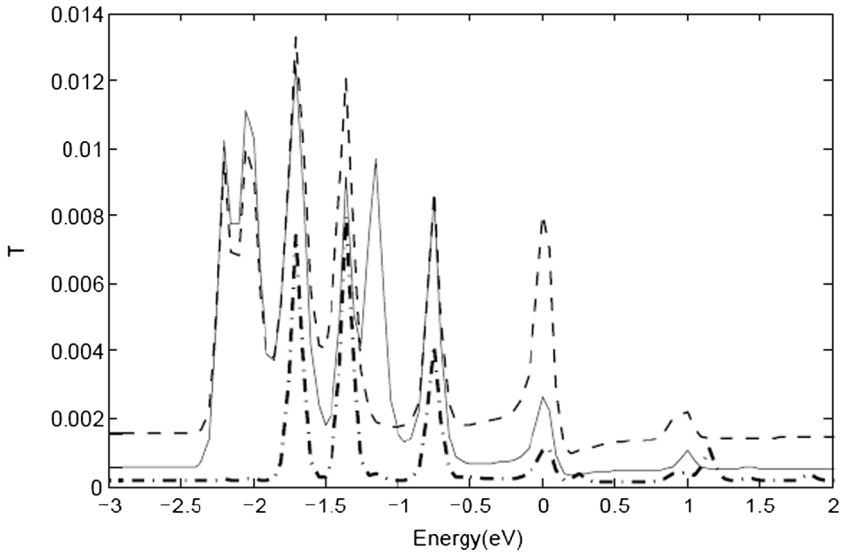

Fig. 3 The total transmission probability of C_{60} molecule as a function of electron energy for one (–.), five(—), and six (__) atomic contacts at V_b=0.0 V and in presence e–p interactions

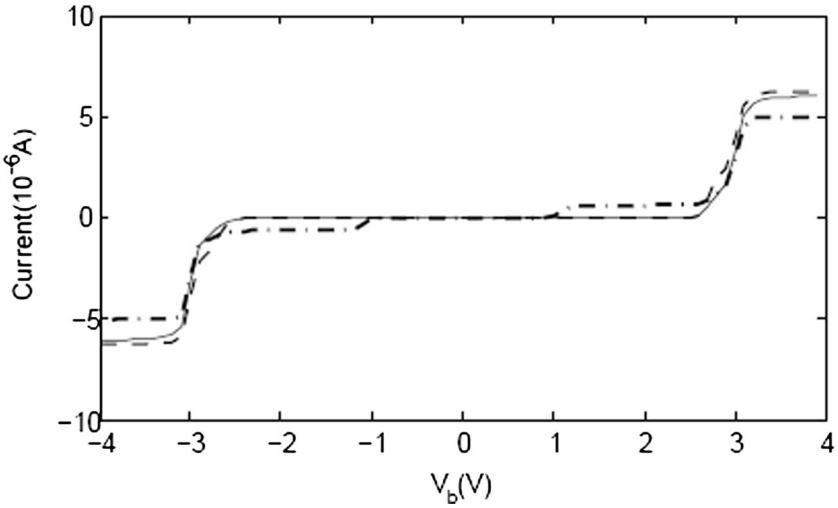

Fig. 4 The electrical current values of C_{60} molecule as a function of bias voltages for one (–.), five(—), and six (__) atomic contacts in absence of e–p interactions

between charge carriers, and the phonon mediated electron–electron interactions are ignored in calculations.

First, our calculations are done with respect to λ=0.2 *eV* and Ω=0.13 *eV*. The total transmission coefficients as a function of the energy of the incident electron for C_{60} molecule are depicted in Fig. 2 in the absence of phonons, with respect to the contact types. The bias voltage is selected V_b=0 V. In the absence of phonons, the three and one resonant tunneling peaks are seen in the cases of single and multiple contacts, respectively.

With the inclusion of phonons, new transmission mechanisms that involve the emission and absorption of phonons are activated. The total transmission spectra as a function of incident electron energy are shown in Fig. 3 with respect to the contact types. The total transmission involves inelastic and elastic interactions, and it is greater than the elastic part. Comparison of Fig. 2 with Fig. 3 indicates that the height of transmission peaks in the presence of electron–phonon coupling is reduced in respect to that in the absence of electron–phonon coupling. Also, there are extra peaks, and the peaks are broadened due to the creation of phonons. Besides, positions of transmission peaks approximately (in Fig. 3) coincide with polaron energies, which are given through the relation:

$$\varepsilon_{pol}(n) = \varepsilon_i + m\Omega - \lambda^2/(\Omega)\ ,$$

where *m* denotes the *m-th* excited state of a polaron and ε_i is corresponding to the molecular level. The main peak corresponds to tunneling through polaron ground state $\varepsilon_{pol}(0)$, while additional side peaks represent next excited states with following energies: $\varepsilon_{pol}(1)$, …, $\varepsilon_{pol}(m_{\max})$, respectively. Moreover, localized electron–phonon interaction leads to the so-called polaron shift $-\lambda^2/\Omega$ which appears as an energy correction for resonant tunneling [25].

With respect to Fig. 3, one can easily observe that the number and height of the transmission resonances increase with increasing number of contact points, respectively.

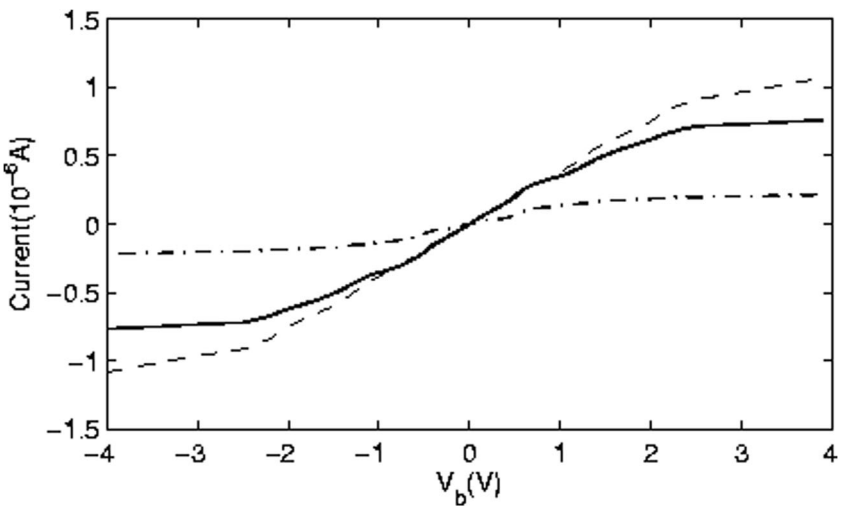

Fig. 5 The total electrical current values of C_{60} molecule as a function of bias voltages for one (–.), five(—), and six (__) atomic contacts in presence of e–p interactions

Also, the peaks are broadened with increasing number of contact points in presence of phonons. On the other hand, the width, the height, and the number of transmission resonances depend on interference effects in quantum transport that is in accordance with other works [28]. The main reason for this is that hybridization with the electrodes is stronger and there are more paths for the electrons to pass through from the metal to the molecule with increasing number of contact points between device electrodes and molecule.

The physical meaning of the interference effect is that the electron waves in the molecule, which come from the different contact points, may undergo a phase shift. Thus, constructive or destructive interference in the propagation process of the electron through the molecule can occur. The effect of the contact is described by the self-energy matrices. Therefore, the Green's function and hence the density of states of the coupled molecule and the transmission spectrum vary with the number of contact points.

It is seen that the value of transmission is small in most of the energy ranges. This is due to the fact that the transmission coefficient depends on two factors of the molecule electronic energy and the electrode/molecule coupling strength. Therefore, the large values of the transmission functions are near the molecular levels of C_{60} where resonance occurs between the incident electron and the molecular level [29].

For cases of single and multiple contacts, the current–voltage (*I-V*) characteristics of C_{60} molecule are shown in Fig. 4 without considering e–p interactions. In these cases, the device is in its off state, and a threshold voltage is needed to generate current through single and multiple contacts of the C_{60} molecule. This is due to the fact that there are no transmission peaks at about the Fermi energy (see Fig. 2). Also, the slight *NDR* behaviors can be seen at high voltages for C_{60} in cases of transport through single and multiple contacts.

Figure 5 describes the current–voltage (*I-V*) characteristics of the C_{60} molecule in cases of transport through single and multiple contacts considering e–p interactions. In these cases, the current–voltage curves do not show off states and *NDR* behavior. Then, e–p interaction is an effective factor on NDR behavior of electronics devices that is similar to other results [18, 30, 31]. Also, total current values considering e–p interactions are smaller than those without considering e-p interactions. Figure 5 shows that the *I-V* characteristics show an Ohmic behavior at low applied voltages for the single and multiple atomic contacts which confirm the simple nonresonant electron tunneling mechanism in these cases [32]. The difference between the *I-V* characteristics in cases with and without considering e–p interactions can be explained with respect to the transmission coefficient peaks.

The *I-V* characteristics of the C_{60} molecule show steplike behavior which is independent of the contact types. The steplike behavior of the *I-V* characteristics can be explained by the curves of the transmission coefficients [see Fig. 2a]. The region of the integral window in the total current integral becomes approximately $[E_F - V_b/2, E_F + V_b/2]$. Furthermore, the total current is equal to the area under the curve of transmission in the region of the integral window. It is evident that the current value increases remarkably when the new transmission peak moves into the integral window with the increase of bias voltage (a new channel is opened). The experimental and theoretical results of the same systems are qualitatively in agreement with present results for the *I-V* characteristics in the cases of single and multiple contacts [33–40].

In Fig. 6, the calculated energy flux is presented against the applied bias voltage in the presence of e–p interactions with respect to contact types. The sign of the energy flux is negative for positive bias voltage because transport is due to the electron conduction through the low unoccupied molecular orbital (LUMO) level of the C_{60} molecule. For the C_{60} molecule, each carbon atom contributes two p state electrons. Therefore, the highest occupied molecular orbital (HOMO) is completely

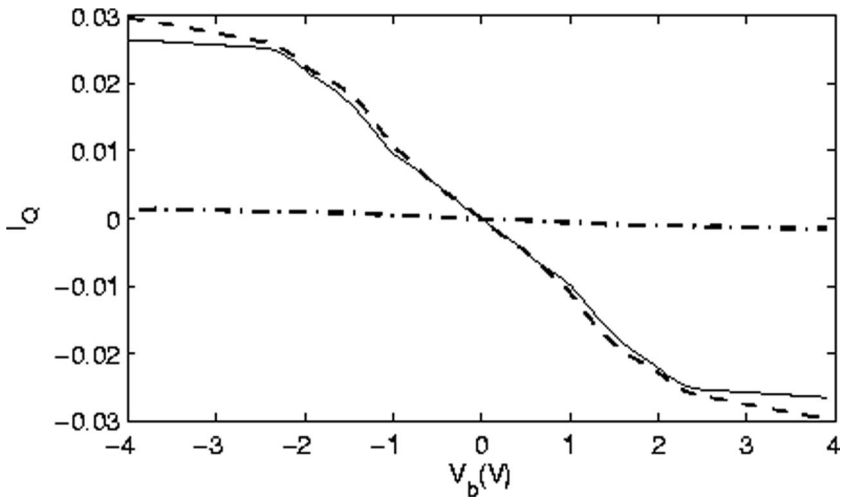

Fig. 6 The energy flux (in unit 2/h) of C_{60} molecule as a function of bias voltages for one (−.), five(−−), and six (__) atomic contacts in presence of e–p interactions

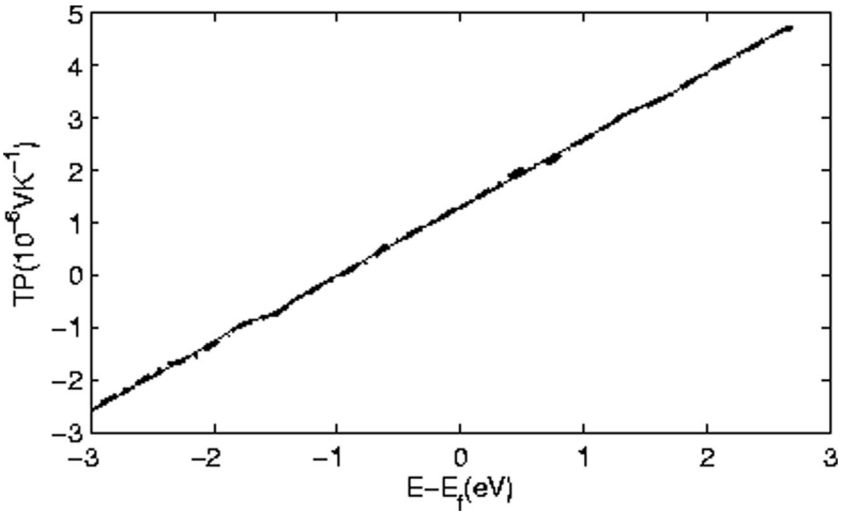

Fig. 7 The total thermopower values of C_{60} molecule as a function of electron energy for one (–.), five(—), and six (__) atomic contacts in absence of e–p interactions

filled, and conduction is done through the LUMO level. In the presence of e–p interactions, the results suggest that the effect of the contact types is dramatic on the current–voltage (*I-V*) characteristic and energy flux of fullerenes. It is seen that the values of current and energy flux with respect to the contact types are ordered as $I_{e/q}(C_1) < I_{e/q}(C_6) < I_{e/q}(C_5)$.

It should be noted that the current from i to j site ($I_{i,j}$) is proportional to $\mathrm{Im}[H_{i,j}G_{i,j}]$ where $H_{i,j}$ represents the Hamiltonian element and $G_{i,j}$ is the electronic relative Green's function between i and j atom sites [41]. Then, electronic transmission depends on bond currents, incident electron in each atom site, and symmetric properties of cages. Therefore, electron conductance and thermoelectric properties of fullerenes vary with respect to the contact types.

Figures 7 and 8 show the thermopower as a function of energy for different contacts in cases with and without considering e–p interactions, respectively. For positive energies, the thermopower sign is positive while for negative energies, it is negative. The mentioned result is independent of the contact types. Figures 7 and 8 show nearly linear trends in the thermopower–energy dependences. However, those trends are characterized by small jumps or small humps. In other words, the thermopower–energy dependence reveals the staircase structure where the number of steps strongly depends on the contact types and presence of e–p interactions.

The first derivatives of thermopowers with respect to energy are presented in Fig. 9. It is clear that any small change in the slope of linear trend of thermopower is viewed as an abrupt jump and hump in its first derivative. Therefore, the numbers of abrupt humps are equal to the numbers of steps. Comparison of Fig. 9 with Fig. 3 indicates that the numbers, width of stairs, and positions of stairs against energy are proportional to that of transmission peaks. On the other hand, the staircase structure of thermopower as a function of energy reveals where transmission values increase. Results indicate that the number of thermopower steps reduce by increasing contact points. Also, the number of thermopower steps in presence of e–p interactions increase with respect to those in

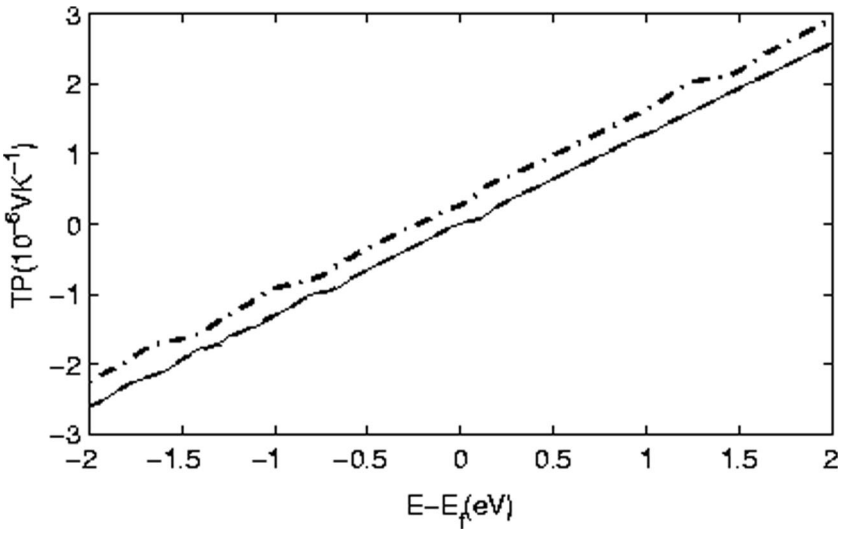

Fig. 8 The total thermopower values of C_{60} molecule as a function of electron energy for one (–.), five(—), and six (__) atomic contacts in presence of e–p interactions

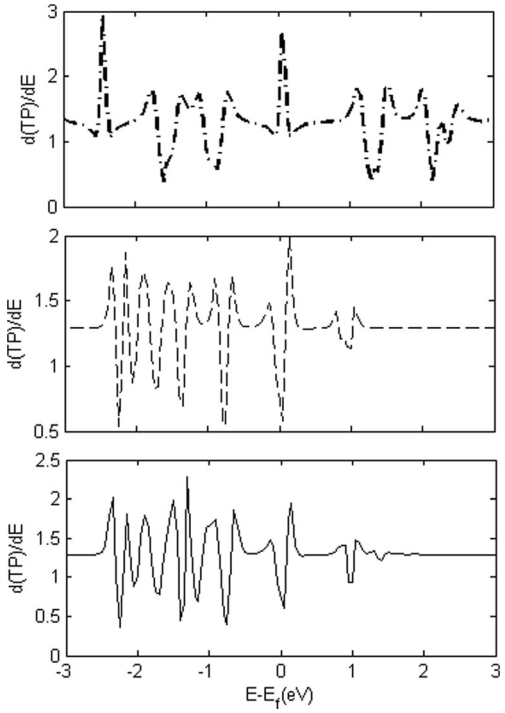

Fig. 9 The first derivatives of total thermopower of C_{60} molecule as a function of electron energy for one (–.), five(—), and six (__) atomic contacts in presence of e–p interactions

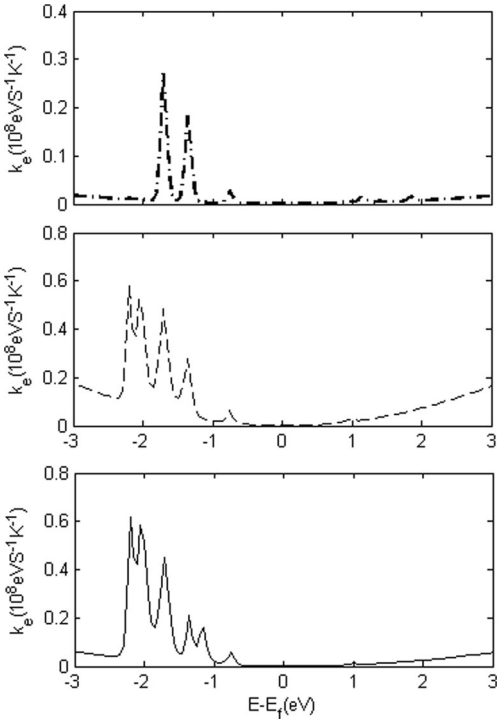

Fig. 11 The total thermal conductance values of C_{60} molecule as a function of electron energy for one (–.), five(—), and six (__) atomic contacts in presence of e–p interactions

absence of e–p interactions because the number of transmission peaks increases when considering e–p interactions. The values of thermopower for the C_{60} molecule are of the order of that for the same system [14, 42, 43].

To get more insight of the thermoelectric properties of the C_{60} molecule, the electronic thermal conductance (k_e) as a function of electron energy has been plotted in Figs. 10 and 11 in absence and presence of phonons, respectively. The electronic thermal conductance behavior is oscillatory for different contacts in case of no e–p interaction. In presence of e–p interactions, the electronic thermal conductance behavior is

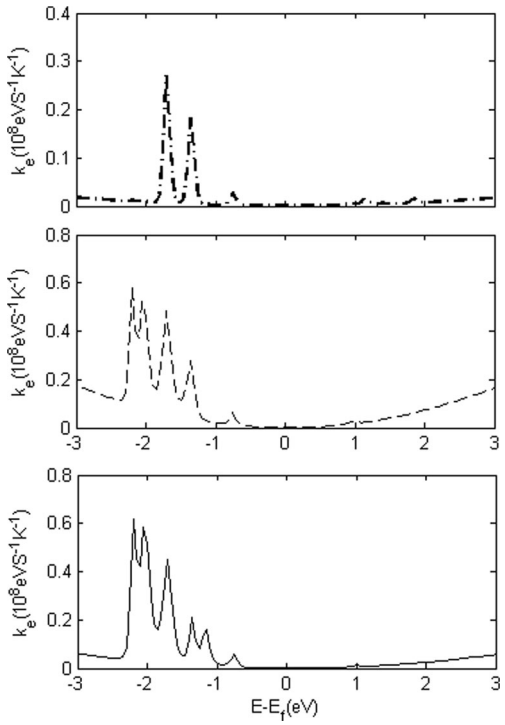

Fig. 10 The total thermal conductance values of C_{60} molecule as a function of electron energy for one (–.), five(—), and six (__) atomic contacts in absence of e–p interactions

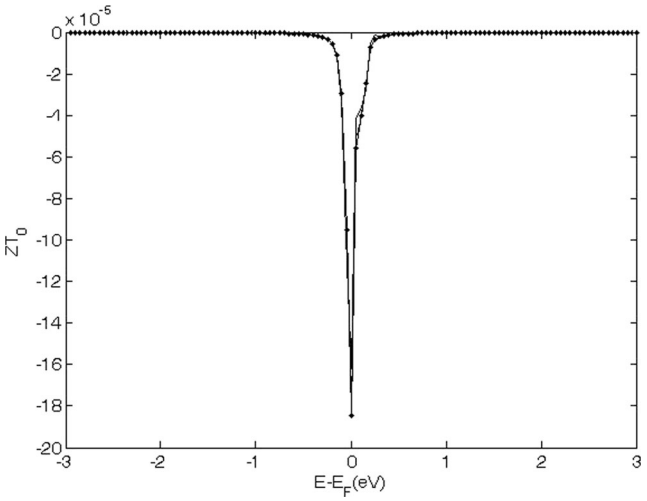

Fig. 12 The merit figure of C_{60} molecule as a function of electron energy for one (–.), five(—), and six (__) atomic contacts in presence of e–p interactions

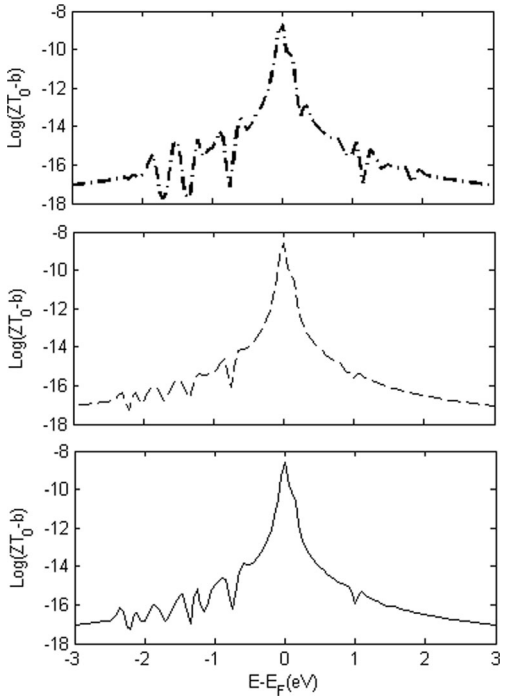

Fig. 13 The merit figure of C_{60} molecule in the logarithmic scale as a function of electron energy for one (−.), five(—), and six (__) atomic contacts in presence of e–p interactions. Here, b is equal to 0.194×10^{-3}

parabolic which is characterized by big oscillations. With comparison of Figs. 10 and 11, one observes that the numbers of peaks in presence of phonons increase with respect to that in absence of phonons. The smallest value of electronic thermal conductance is belonging to the single atomic contact and the biggest value ($k_{e\max}$) of it is belonging to the six atomic contacts. The maximum value of electronic thermal conductance for multiple contacts about is two times bigger than that for one atomic contact. Also, the peak position of $k_{e\max}$ via energy in presence and absence of phonons is different for one and multiple contacts. By using first-principle calculations, the origin of the oscillatory behavior of the thermal conductance is attributed to filling of the p states of carbon chains [44]. It is clear that the elastic part values of electronic thermoelectric are smaller than that for the inelastic part. The $k_{e\max}$ in presence of e–p interactions dramatically decrease relative to that in absence of e–p interactions, so that ratio of $k_{e\max}$ in absence of e–p interactions to it in presence of e–p interactions is more than 100.

In presence of e–p interactions, the figures of merit ($ZT_0 = \frac{G_e S^2 T}{k_e}$) via energy for C_{60} molecule have been plotted in Fig. 12 with respect to contact types. There is significant interest in improving figures of merit in thermoelectric materials for many industrial and energy applications. All the figures of merit as functions of energy are very similar at first glance and show characteristic minimum exactly at the Fermi energy. This problem could be solved by presenting Fig. 12 in the logarithmic scale within energy range between −3 and 3.

Figure 13 shows that the behavior ZT_0 is oscillatory with respect to contact types. The values and behavior of ZT_0 are dependent on the contact types. The minima (dips) of the dimensionless figures of merit at around Fermi energy are typically an order of magnitude smaller than the other values of considered quantities. Since the Fermi energy of contacts is an important parameter for transport properties of molecular junctions, therefore, contact properties have dominant influence on the shape of thermoelectric characteristics of the fullerene junctions. The minimum values of ZT_0s are equal to 3.167×10^{-5}, 1.17×10^{-5}, and 9.01×10^{-6} for one, five, and six atomic contacts, respectively.

Finally, the *I-V* characteristics of the C_{60} molecule are shown in Fig. 14 for $\Omega = 0.10 eV$ in case of one atomic contact. It is clear that the values of λ and Ω are important factors in calculations.

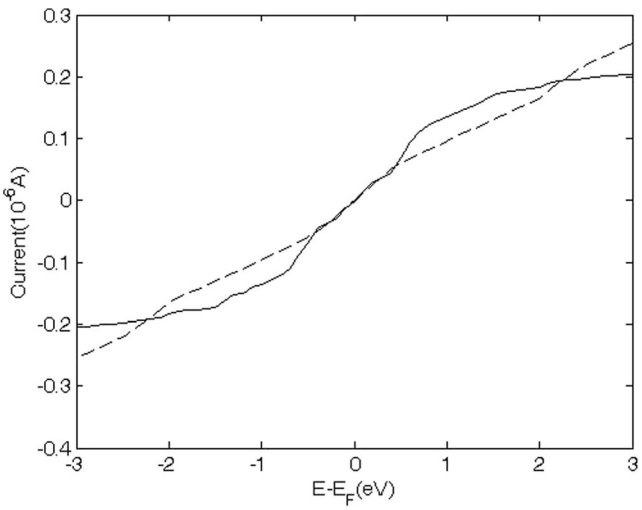

Fig. 14 The total electrical current values of C_{60} molecule as a function of bias voltages for $\Omega = 0.013 eV$ (__) and $\Omega = 0.010 eV$(− −)

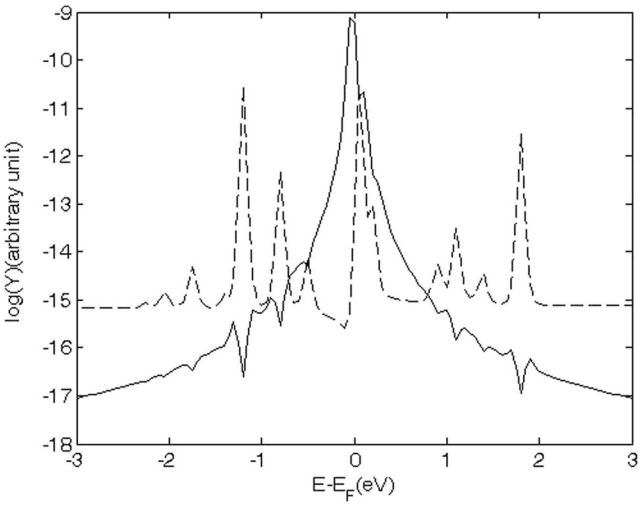

Fig. 15 The total transmission probability (—) and merit figure (ZT) (__) of C_{60} molecule in logarithmic scale as a function of electron energy for $\Omega = 0.010 eV$

Also, Fig. 15 presents ZT_0 and electrical conductance of C_{60} in the logarithmic scale for $\Omega = 0.10 eV$. In case of one atomic contact, the minimum value of ZT_0 of C_{60} is equal to 8.55×10^{-5} for $\Omega = 0.10 eV$ which is of order of that for $\Omega = 0.13 eV$. As shown in Fig. 15, small ZT_0s occur only at the sides of resonances of conductance, and ZT_0 dramatically decreases at exact resonance positions of conductance about Fermi energy. In other words, combined effect of discreteness of molecular energy levels and local interactions between electrons and phonons are important in determining thermoelectric properties. Therefore, frequency of oscillations for ZT_0s corresponds to frequency of phonon involved in the conduction process, and polaron-type oscillations are somehow related to phonon-assisted transport channels. With respect to contact types and values of λ and Ω, the values of ZT_0s change in the interval $[0.322 \times 10^{-7}, 0.194 \times 10^{-3}]$.

Undeniably, the energy-dependent oscillations of dimensionless figure of merit and the thermoelectric properties of molecules on both sides around the Fermi energy are due to the fact that most of the current is carried by electrons with Fermi energy. Overall, the mentioned phenomena are in association with a combined effect of discreteness of molecular energy levels and local interactions between electrons and phonons (i.e., individual processes of phonon emission or absorption).

4 Conclusions

A theoretical analysis of inelastic and different contact geometry effects on electron transport and thermoelectric properties of C_{60} in both linear and nonlinear response regimes have been performed. The WB approximation and GFT-PT which maps the many-body electron–phonon interaction problem into a one-body multichannel single-electron scattering problem have been used in this work. The results present that the transmission curves and the I-V characteristics calculated at the single and multiple couplings to the electrodes can be completely different due to the interference effects.

In addition, the influence of e–p interactions for the C_{60} molecule is observed as the dramatic decrease in values of transmission peaks, current and the electronic thermal conductance. Besides, combined effect of discreteness of molecular energy levels and individual processes of phonon emission or absorption of transport are important factors in thermoelectric and transport properties of the C_{60} molecule.

References

1. T.-H. Park, M. Galperin, Phys. Scr. T **151**, 014038 (2012)
2. M.A. Reed, C. Zhou, C.J. Muller, T.P. Burgin, J.M. Tour, Science **278**, 252 (1997)
3. R.H.M. Smit, Y. Noat, C. Untiedt, N.D. Lang, M.C. van Hemert, J.M. van Ruitenbeek, Nature **419**, 906 (2002)
4. L.A. Bumm, J.J. Arnold, M.T. Cygan, T.D. Dunbar, T.P. Burgin, L. Jones II, D.L. Allara, J.M. Tour, P.S. Weiss, Science **271**, 1705 (1996)
5. S. Yamacli, Phys. Scr. **82**, 045705 (2010)
6. B.N.J. Persson, N.G. van Kempen, Phys. Scr. **38**, 282 (1988)
7. F. Cataldo, G. Strazzulla, S. Iglesias-Groth, Mon. Not. R. A.stron Soc **394**, 615 (2009)
8. L.S. Wang, J.M. Alford, Y. Chai, M. Diener, J. Zhang, S.M. Mcclure, T. Guo, G.E. Scuseria, R.E. Smalley, Chem. Phys. Lett. **207**, 354 (1993)
9. D. Zhang, J. Wu, J. Kong, J. Yan, Chin. Phys. Lett. **10**, 143 (1993)
10. W.J. Liang, M.P. Shores, M. Bockrath, J.R. Long, H. Park, Nature **417**, 725 (2002)
11. S.M. Sze, *Physics of Semiconductor Devices*, 2nd edn. (Wiley, New York, 1981)
12. L.L. Chang, E.E. Mendez, C. Tejedor, *Resonant Tunneling in Semiconductors* (Plenum Press, New York, 1991)
13. S. Datta, *Electronic Transport in Mesoscopic System* (Cambridge University Press, Cambridge, 1995)
14. J. Hone, I. Ellwood, M. Muno, A. Mizel, M.L. Cohen, A. Zettl, A.G. Rinzler, R.E. Smalley, Phys. Rev. Lett. **80**, 1042 (1998)
15. R.T. Littleton, T.M. Tritt, J.W. Kolis, D.R. Ketchum, Phys. Rev. B **60**, 13453 (1999)
16. S.J. Youn, A.J. Freeman, Phys. Rev. B **63**, 085112 (2001)
17. A.G. Pogosov, M.V. Budantsev, D. Uzur, A. Nogaret, A.E. Plotnikov, A.K. Bakarov, A.I. Toropov, Phys. Rev. B **66**, 201303 (2002)
18. T. Koch, H. Fehske, J. Loos, Phys. Scr. **151**, 014039 (2012)
19. B. Ludolph, J.M. van Ruitenbeek, Phys. Rev. B **59**, 12290 (1999)
20. N.J. Appleyard, J.T. Nicholls, M. Pepper, W.R. Tribe, M.Y. Simmons, D.A. Ritchie, Phys. Rev. B **62**, R16275(R) (2000)
21. K.A. Matveev, A.V. Andreev, Phys. Rev. B **66**, 045301 (2002)
22. T. Smith, M. Tsaousidou, R. Fletcher, P.T. Coleridge, Z.R. Wasilewski, Y. Feng, Phys. Rev. B **67**, 155328 (2003)
23. E. Emberly, G. Kirczenow, Landauer theory. Phys. Rev. B **61**, 5740 (2000)
24. N. Kurita, K. Kobayashi, H. Kumahora, K. Tago, Phys. Rev. B **48**, 4850 (1993)
25. K. Walczak, Physica B **392**, 173 (2007)
26. Y. Asai, H. Fukuyama, Phys. Rev. B **72**, 085431 (2005)
27. G.D. Guttman, E. Ben-Jacob, D.J. Bergman, Phys. Rev. B **51**, 17758 (1995)
28. L. Wang, K. Tagami, M. Tsukada, Jpn. J. Appl. Phys. **43**, 2779 (2004)
29. A. Saffarzadeh, J. Appl. Phys. **103**, 083705 (2008)
30. P. Zhao, D.S. Liu, Y. Zhang, Y. Su, S.J. Li, G. Che, Phys. Lett. A **375**, 2639 (2011)
31. X. Zheng, W. Lu, T.A. Abtew, V. Meunier, J. Bernholc, ACS Nano **4**, 7205 (2010)
32. J. Guo, *Carbon nanotube electronics: modeling, physics, and applications* (PhD Thesis,Purdue University, 2004)
33. C. Joachim, J.K. Gimzewski, Europhys. Lett. **30**, 409 (1995)
34. D. Porath, Y. Levi, M. Tarabiah, O. Millo, Phys. Rev. B **56**, 9829 (1997)
35. D. Porath, O. Millo, J. Appl. Phys. **81**, 2241 (1997)
36. B. Huang, J. -x. Zhang, R. Li, Z. -y. Shen; S.-m. Hou; X. Zhao; Z. -q. Xue; Q. -d. Wu, *Acta Phys. Chim. Sin.*, **22**, 161 **(2006)**
37. G.J. Tian, W.Y. Su, Chin. Phys. Lett. **26**, 068501 (2009)
38. M. Paulsson, S. Stafström, J. Phys, Condens. Matter **11**(3555) (1999)
39. J. Taylor, H. Guo, J. Wang, Phys. Rev. B **63**, 245407 (2001); Phys. Rev. B **63**, 121104(R) (2001)
40. G. Géranton, C. Seiler, A. Bagrets, L. Venkataraman, F. Evers, J. Chem. Phys. **139**, 234701 (2013)
41. C.W.J. Beenakker, H. von Houten, *Solid State Physics, Semiconductor Heterostructures and Nanostructures* (Academic, New York, 1991)
42. Y.W. Park, Synth. Met. **45**, 173 (1991)
43. J. Vavro, M.C. Llaguno, B.C. Satishkumar, D.E. Luzzi, J.E. Fischer, Appl. Phys. Lett. **80**, 1450 (2002)
44. N.D. Lang, P. Avouris, Phys. Rev. Lett. **81**, 3515 (1998)